Available online at www.sciencedirect.com
SCIENCE DIRECT
Nuclear Instruments and Methods in Physics Research A 558 (2006) 536–541
NUCLEAR INSTRUMENTS & METHODS IN PHYSICS RESEARCH Section A
www.elsevier.com/locate/nima

Improved PID method of temperature control for adiabatic demagnetization refrigerators

A. Hoshino[a,*], K. Shinozaki[a], Y. Ishisaki[a], T. Mihara[b]

[a]*Department of Physics, Tokyo Metropolitan University, Minami-Osawa 1-1, Hachioji, Tokyo 192-0397, Japan*
[b]*RIKEN, Hirosawa 2-1, Wako, Saitama 351-0198, Japan*

Received 25 July 2005; received in revised form 11 December 2005; accepted 11 December 2005
Available online 4 January2006

Abstract

We report a new method of precise temperature control for an adiabatic demagnetization refrigerator (ADR). Temperature of the experimental stage of ADRs is usually controlled with the standard PID (Proportional, Integral, and Derivative control) method by decreasing the magnet current of the superconducting solenoid surrounding the paramagnetic salt inside the ADR. In controlling the temperature of our portable ADR system, we found a small residual between the aimed and measured temperatures, which gradually increased in time as the magnet current decreases. This phenomenon is explained by the magnetic cooling theory, and we have introduced a new functional parameter to improve the standard PID method. Applying this improvement to our system, highly stabilized temperature of 10 μK rms at 100 mK up to the period of ~15 ks is presented. It is demonstrated that the temperature controlled time was increased by ~30% in our experiment. Our improved PID method is useful to maintain the long-term temperature stability down to almost zero magnet current with a relatively small ADR.

PACS: 07.05.Dz; 95.55.Ka

Keywords: Control system; Low temperature; Magnetic cooling; PID; ADR

1. Introduction

The high resolution X-ray spectroscopy with a non-dispersive instrument is strongly desired in the X-ray astronomy field [1] because dispersive instruments with Bragg crystals or gratings have generally low throughputs and are not usable with extended sources. The single-photon microcalorimeter is one of the best candidates which realizes a spectral resolution comparable to dispersive instruments. The first results are reported for a sounding rocket experiment [2], and also Japanese X-ray astronomy satellite, *Suzaku* (formerly called Astro-E2) with the XRS instrument has realized $E/\Delta E \sim 1000$ at 6 keV in orbit [3]. Such high spectral resolution with a compact system is also attractive to the industrial and laboratorial applications, e.g., material analysis, plasma diagnostics, etc. [4]. The recent inventions of superconductive transition-edge sensor (TES) calorimeters [5] and metallic magnetic calorimeters (MMC) [6] has accelerated this stream.

However, all these kinds of calorimeters require extreme low temperature well below ~100 mK and simultaneously the highest temperature stability $\Delta T/T$ typically better than the energy resolution $\Delta E/E$. For example, the refrigerator of the *Suzaku* XRS is specified to maintain the temperature of 60 mK to be better than 10 μK rms over a 10 s to 10 min timescale. In the space environment, an adiabatic demagnetization refrigerator (ADR) is an almost unique and ideal solution, since it is all solid, and properly works on zero-g condition in contrast to the dilution refrigerator commonly used in the ground experiment. It is also possible to make the ADR relatively compact and portable. The ADR makes use of the magnetic cooling, allowing the spins of electrons in a paramagnetic salt to randomize adiabatically in a small magnetic field, which is

*Corresponding author. Tel.: +81 426 77 2492; fax: +81 426 77 2483.
E-mail address: h_akio@phys.metro-u.ac.jp (A. Hoshino).

0168-9002/$ - see front matter © 2005 Elsevier B.V. All rights reserved.
doi:10.1016/j.nima.2005.12.046

once aligned under the strong magnetic field (see Ref. [7] for review). It is also a merit of the ADR that the temperature can be controlled quite precisely by controlling the current of superconducting magnet surrounding the salt. On the other hand, when the magnetic spins are completely randomized, i.e., no more heat can be absorbed, a "recharge" of the refrigerator is necessary. The period to the next recharge, i.e., temperature controlled time, depends on the heat input to the salt, the temperature to maintain, and the size of the salt.

We have also developed a portable ADR system for ground experiments [4], which is based on the system originally designed for the rocket experiment [2]. While developing a compact and portable ADR, we faced a problem limiting the temperature controlled time in the cooling cycle. Because heat capacity of the refrigerant material in a "salt pill" is small for compact ADRs, difficulties arises in keeping constant temperature for a long time. Particularly, we found small residual temperature difference between the aimed and measured temperatures, which gradually increased in time when we controlled the temperature of our ADR with the standard PID (Proportional, Integral, and Derivative control) method. The problem originates in the principle of the standard PID which is naively applied to ADRs, making it critical to keep stable temperature with a small refrigerator. Bernstein et al. [8] have demonstrated quite steady control of the ADR temperature by rejecting thermometry readout noise and optimizing varying parameters which determine $\mathrm{d}I/\mathrm{d}t$, although their method assumes the magnet current, I, is sufficiently high. We have succeeded in solving the problem with an improved PID method by adding a new term in the standard PID considering the physical properties of the paramagnetic salt, and demonstrated it with our portable ADR system. In this article, we introduce the outline of the improved PID method, and the experimental results with our ADR system are presented.

2. Theory of temperature control method and magnetic materials

2.1. PID method

With regard to usual refrigeration systems which have a cold bath and an experimental stage equipped with a resistive heater, the temperature, T, of the experimental stage is usually controlled by the heater output, $w(t)$, in dimension of W, making use of the standard PID method. In this case, heat load on the experimental stage, $w_{\mathrm{L}}(t)$, and the heat outflow into the cold stage, $w_{\mathrm{out}}(t)$, should be balanced with $w(t)$, as

$$\overline{w(t)} + \overline{w_{\mathrm{L}}(t)} = \overline{w_{\mathrm{out}}(t)} \tag{1}$$

in which $\overline{w(t)}$ represents the time average of $w(t)$. Here, $w_{\mathrm{L}}(t)$ is almost constant with a small level of fluctuations, and the $w_{\mathrm{out}}(t)$ is determined by the thermal conductivity and the temperature difference between the experimental stage and the cold bath. In the standard PID method, the $w(t)$ is determined with a formula,

$$w(t) = \frac{\mathscr{I}}{\Delta t}\int_{t-\Delta t}^{t} w(t')\,\mathrm{d}t' - \mathscr{P}\{T(t) - T_{\mathrm{aim}}\} - \mathscr{D}\frac{\mathrm{d}T}{\mathrm{d}t}(t) \tag{2}$$

in which T_{aim} is the aimed temperature to maintain, and $\mathscr{P}$, $\mathscr{I}$, $\mathscr{D}$, Δt are the non-negative constant parameters. The first term with $\mathscr{I} \simeq 1$ represents the constant heater output when perfectly $T = T_{\mathrm{aim}}$, and the second or third term indicates the compensational heater output proportional to the difference or differential of the measured temperature, respectively.

On the other hand in the ADR systems, the experimental stage is stiffly connected to the refrigerant salt itself, so that the temperature, T, of the experimental stage is almost equivalent with the temperature of the salt pill. We can control the heat absorption, $w_{\mathrm{a}}(t)$ in the salt pill by changing the current, $i(t)$, of the superconducting solenoid magnet. It is also notable that warming and cooling are both feasible with ADRs by increasing or decreasing the current, while resistive heaters can do only warming. Fig. 1 represents a schematic example of the temperature control with ADRs. Each of solid lines indicates the entropy behavior under a certain constant magnetic field, plotted versus temperature. The magnetic field is weaker for upper lines. Under the constant magnetic fields of $B(1)$, the temperature slowly increase due to the heat input $w_{\mathrm{in}}(t)$ from the bottom point towards the upper-right direction along the solid line. At some point where the temperature difference is significant, the magnetic field is reduced to $B(2)$ by decreasing the magnet current and the state of the ADR jumps to the upper solid line. This step occurs in a short time scale through closely adiabatic path, so that the entropy, S, is preserved and the temperature is lowered. Repeating these steps with sufficient minuteness, the temperature of the ADR salt can be controlled quite

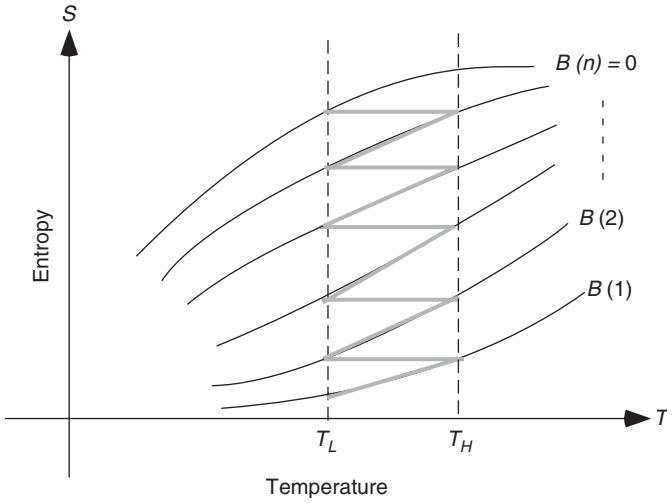

Fig. 1. A schematic example of temperature control with ADRs, plotted on the entropy–temperature plane. Each of solid lines indicates the entropy behavior of the paramagnetic salt under a certain constant magnetic field. See text for details.

precisely, usually to the level of the temperature determination accuracy. Ideally, we can control the temperature until the magnet current, $i(t)$, reaches down to zero.

In order to stabilize the ADR temperature, the equation to balance is,

$$\overline{w_{\mathrm{a}}(t)} = \overline{w_{\mathrm{in}}(t)} \tag{3}$$

while $w_{\mathrm{a}}(t)$ is a complicated function of B, T, and other ADR specific parameters, as described in the next subsection. Therefore, the easiest way of incorporating the PID method to ADRs is to replace $w(t)$ in Eq. (2) with $i(t)$. There is a similarity between $w(t)$ and $i(t)$ that increasing (or decreasing) the value corresponds to raising (or lowering) the temperature. One difference is, however, that $i(t)$ must be decreased gradually to zero, in long-range time scale. In order to take into account this effect, we have introduced another term, $F(t)$, into Eq. (2) as,

$$i(t) = \frac{\mathscr{I}}{\Delta t}\int_{t-\Delta t}^{t} i(t')\,\mathrm{d}t' - \mathscr{P}\{T(t) - T_{\mathrm{aim}}\} - \mathscr{D}\frac{\mathrm{d}T}{\mathrm{d}t}(t) + F(t). \tag{4}$$

Throughout this article, we call the temperature control method based on this equation with $F(t)\neq 0$ as an improved PID method, and the method with $F(t) = 0$ as the standard PID method. Considering the fact that the first term roughly equal to $(i(t) + i(t-\Delta t))/2$ when $\mathscr{I} = 1$, $F(t)$ should follow

$$F(t) \simeq \frac{i(t) - i(t-\Delta t)}{2} \simeq \left(\frac{\Delta t}{2}\right)\frac{\mathrm{d}i}{\mathrm{d}t}(t) \tag{5}$$

ignoring the second and third term. Because $i(t)$ gradually decreases, $F(t)$ is always negative. This value is usually small compared with the fluctuation of the actual setting of $i(t)$, hence it is not realistic to determine $F(t)$ at each time by numerically differentiating $i(t)$. To specify the functional form of $F(t)$, help of the theory on magnetism.

2.2. Magnetic theory

In this subsection, we deal with the physical property of the localized spin in the magnetic material, and derive a simple formula balancing the heat input, w_{in}, and the heat absorption, w_{a}, in the salt pill. Typically, a 3d-group transition metals or rare earth elements which has unpaired electrons in the outer shell are utilized as the magnetic material of ADRs. The total angular momentum quantum number J of the localized spin is expressed with a sum of spin angular momentum S and orbital angular momentum L (LS-coupling). In the applied magnetic field of B at the temperature of T, the magnetization $M(T,B)$ for the N spin system is represented by a Brillouin function as

$$M(T,B) = Ng\mu_{\mathrm{B}}J\left\{\frac{2J+1}{2J}\coth\left(\frac{2J+1}{2J}x\right) - \frac{1}{2J}\coth\left(\frac{x}{2J}\right)\right\} \tag{6}$$

in which $x \equiv g\mu_{\mathrm{B}}BJ/k_{\mathrm{B}}T$, g is the Landé factor, μ_{B} is the Bohr magneton, and k_{B} is the Boltzmann constant. Then the magnetic entropy, $S(T,B)$, is,

$$S(T,B) = Nk_{\mathrm{B}}\ln(2J+1) + \int_0^B \left(\frac{\partial M}{\partial T}\right)_{B'}\mathrm{d}B'. \tag{7}$$

In fact, B is the magnetic field which contributes to the spin, and is represented by the superposition of the internal spin b and the external field B_0, as

$$B = \sqrt{b^2 + B_0^2}. \tag{8}$$

When the thermal energy is dominant, namely $x \ll 1$,

$$M(T,B) = \frac{CB}{\mu_0 T}, \quad C = \frac{N\mu_0 g^2\mu_{\mathrm{B}}^2 J(J+1)}{3k_{\mathrm{B}}}. \tag{9}$$

The former equation in Eq. (9) is known as the Curie's law, and C is the Curie constant. As a result, Eq. (7) of the entropy is reduced to

$$S(B,T) = Nk_{\mathrm{B}}\ln(2J+1) - \frac{CB^2}{2\mu_0 T^2}. \tag{10}$$

We must pay attention to the condition that $x \ll 1$. This means that the thermal energy, $k_{\mathrm{B}}T$, is much higher than the magnetic energy, $g\mu_{\mathrm{B}}BJ$.

2.3. Heat balance during the temperature control

To make it simple, the heat inflow, w_{in}, is assumed to be constant. The thermal energy due to w_{in} during the time δt is $w_{\mathrm{in}}\delta t$. This energy input must be balanced with the heat absorption in the salt pill, $w_{\mathrm{a}} = T\delta S$. Here we put $B_0 = c_1 i$, and using Eqs. (8) and (10), then we derive

$$w_{\mathrm{in}}\delta t = w_{\mathrm{a}}\delta t = T\delta S = -\frac{c_1^2 C}{\mu_0 T}\,i\,\delta i \tag{11}$$

in which the internal field, b, is cancelled out. Therefore,

$$\frac{\mathrm{d}i}{\mathrm{d}t}(t) = -\frac{\mu_0 w_{\mathrm{in}} T}{c_1^2 C}\frac{1}{i(t)} = -\frac{\mathscr{A}^2}{2}\frac{1}{i(t)} \tag{12}$$

in which $\mathscr{A} \equiv \sqrt{2\mu_0 w_{\mathrm{in}} T/(c_1^2 C)}$. Combining Eqs. (4), (5), and (12), formula of the improved PID method can be written as,

$$i(t) = \frac{\mathscr{I}}{\Delta t}\int_{t-\Delta t}^{t} i(t')\,\mathrm{d}t' - \mathscr{P}\{T(t) - T_{\mathrm{aim}}\} - \mathscr{D}\frac{\mathrm{d}T}{\mathrm{d}t}(t) - \frac{\mathscr{A}^2\Delta t}{4i(t)}. \tag{13}$$

3. Experiment

3.1. Setup

We have done simple experiments to verify our formulation of the improved PID method with our portable ADR system. The details of the system are described in Ref. [4]. The experimental setup and several parameters of the refrigerator are shown in Fig. 2 and Table 1. We stabilized temperature of the experimental stage by controlling the current of the superconducting solenoid magnet according to Eq. (13). The

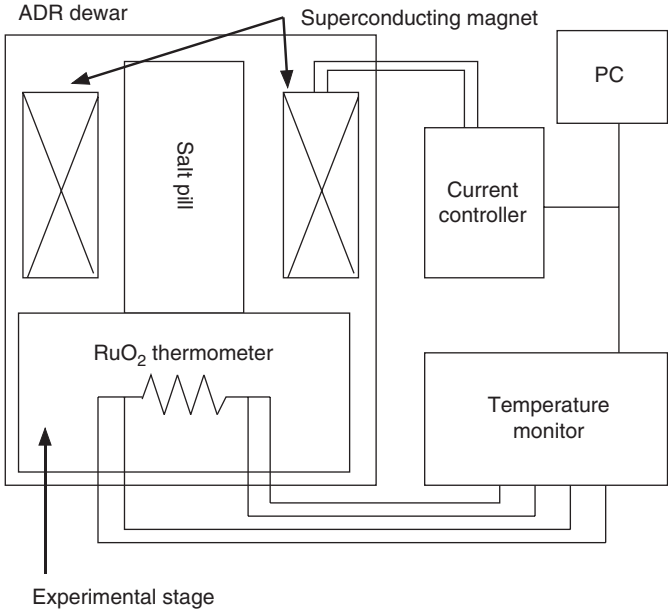

Fig. 2. A block diagram of temperature control experiments with our ADR system.

Table 1
Setup parameters of the ADR in the experiments

Aimed temperature to maintain	100 mK
Heat inflow at 100 mK	0.6–0.8 μW
Paramagnetic material	FAA (0.187 mol)
Heat capacity at 100 mK	3.3 J K^{-1} mol^{-1}
Heat sink temperature (pumped liquid ^{4}He)	1.7 K

temperature was monitored with the RuO_2 (Ruthenium-Oxide) thermometer attached on the experimental stage. The thermometer resistance was measured using the temperature monitor, Cryo-con Model 62, with the four wire connection, and the filter time constant was set to 8 s. The inherent noise of the thermometer bridge is measured as rms = 5.0 μK with a constant resistor placed at 100 μK in the ADR. The self-heating of the thermometer is less than 1 pW, which is much smaller than the heat inflow (Table 1), and the temperature difference between the thermometer and the experimental stage is negligible. The magnet current was controlled by the current controller, Keithley 2400, with the finest resolution of 5 μA. Both the temperature monitor and the current controller were connected to a laptop computer (PC) with GPIB bus, which conducted the temperature control according to the PID calculations.

The operation of the temperature control was done in the 1 s cycle, although the thermal time constant between the experimental stage and the salt pill is less than 1 s. Namely, the temperature acquisition, calculation, and setting of the new magnet current were done at every 1 s. In order to calculate the next magnet current, $i(t+\Delta t)$, one needs the temperature, $T(t)$, the temperature differentiation, $dT/dt(t)$, and the magnet current, $i(t)$, in Eq. (13). These values tend to be affected by noises in actual situations, therefore we averaged these values in the previous 60, 15, and 15 samples, respectively. The superconducting solenoid magnet has a thermal link to the pumped liquid ^{4}He bath at 1.7 K, and the maximum magnetic field is 2.85 T at the magnet current of $i = 5.5$ A. There is a backing coil in the solenoid coil to cancel the magnetic field at the experimental stage, which also has a cryoperm shield to further reduce the magnetic effects. Although the RuO_2 thermometer is little affected by the magnetic field, that on the experimental stage is less than 1 G during the temperature control.

We utilizes 89.8 g of FAA (ferric ammonium alum; $Fe(NH_4)(SO_4)_2 \cdot 12H_2O$) for the magnetic cooling material, and it is sealed in the salt pill. The heat capacity of the other components attached to the salt pill is quit smaller than that of FAA at the lowest temperature. The salt pill is suspended by six Kevler supports. Because the hold time of the pumped liquid ^{4}He is ~24 h, which is sufficiently longer than the temperature controlled time of the cold part at 100 mK in the single ADR cycle, the heat inflow to the cold part can be regarded to constant (0.6–0.8 μW at 100 mK). The FAA crystal, however, has become slightly deteriorated, the internal field, b, in our FAA salt is somewhat larger than that of a complete FAA crystal.

3.2. Result

The temperature control results with the standard PID and the improved PID method are shown in Fig. 3. In these experiments, the parameters for the improved PID method are summarized in Table 2, in which we added a small offset, $i_{off} = 2.5$ mA, to the magnet current, $i(t) \equiv i_m(t) + i_{off}$, to avoid the divergence of the term $(\mathscr{A}^2\Delta t)/4i(t)$ to infinity when $i(t) \to 0$. Here, $i_m(t)$ is the actual current set by the current controller. After ~10 ks when the magnet current becomes lower than ~30 mA, the difference between the two is noticeable. In the improved PID method (Fig. 3(a)), it keeps constant temperature at 100 mK, while the temperature begins to rise in the standard PID method (Fig. 3(b)). The mean temperature of the improved PID is well consistent with the aimed temperature of 100 mK, while it is significantly shifted by ~20 μK with the standard PID (Fig. 3(d)). The temperature dispersion in the whole time range is by about 1.5 times smaller for the improved PID with rms = 11.0 μK. In addition, the magnet current for the improved PID ramps down to zero slower than that for the standard PID (Fig. 3(c)). It might be suggested that the eddy-current heating were reduced due to smoother temperature control. The two experiments were conducted in the same day without warming up the cryostat, it is unlikely that the parasitic heat leak had changed between the two. We have cooled our ADR system more than 100 times since 2002, and the reproducibility of the ramping time was typically ~10%. In this respect, however, the difference is not significant.

The temperature dispersion in a shorter time scale between 2000–4000 s is derived to be rms = 9.4 μK for

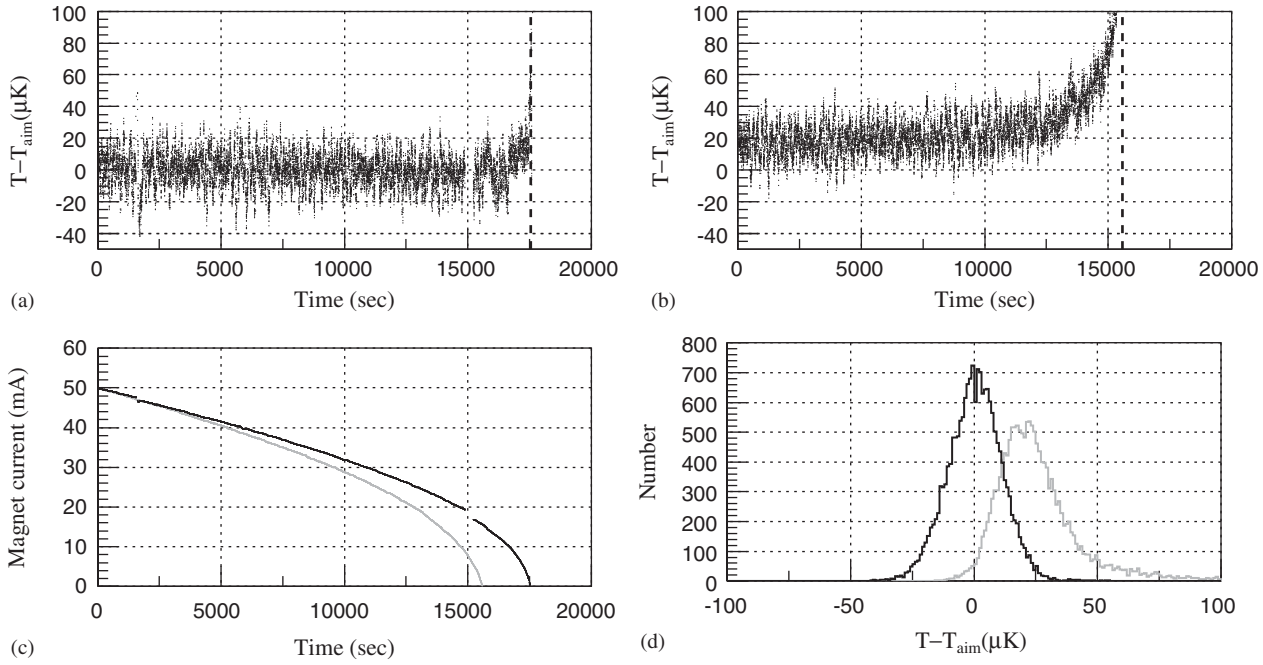

Fig. 3. Results of the temperature control experiments with the aim of temperature $T_{\rm aim} = 100\,{\rm mK}$ to maintain. (a) The measured temperature residual, $T - T_{\rm aim}$, in unit of μK plotted versus time in seconds with the improved PID method. (b) Similar to (a) with the standard PID method. (c) The magnet current, $i_{\rm m}(t)$, in unit of mA plotted versus time in seconds. The solid black line represent the magnet current with the improved PID, and the gray line is that with the standard PID. (d) Histograms of the residual temperature at each second for both methods in the whole time range plotted in (a) and (b). Regarding the improved PID (black), mean of the temperature residual is 0.3 μK and rms is 11.0 μK in the whole time range. For the standard PID (gray), mean is 25.1 μK and rms is 16.3 μK.

Table 2
The PID parameters for the experiment

$\mathscr{P}$	114 [mA K^{-1}]
$\mathscr{I}$	1.0
$\mathscr{D}$	5500 [mA K^{-1} s]
$\mathscr{A}$	0.544 [mA s$^{-1/2}$]
$i_{\rm off}$	2.5 [mA]
Δt	1.0 [s]

Table 3
Parameters in calculating the predicted value of $\mathscr{A}$

Curie's constant for FAA ($g = 2$, $J = 5/2$)	$C = 43.8\,\mu_0$ [J K T^{-2} mol^{-1}]
Aimed temperature	$T = 100$ [mK]
Heat inflow	$w_{\rm in} = 0.6$–0.8 [μW]
External magnetic field per unit current	$c_1 = 0.518$ [TA^{-1}]
Predicted value	$\mathscr{A} = 0.234$–0.270 [mA s$^{-1/2}$]

the improved PID and rms = 9.9 μK for the standard PID, both of which is close to but slightly above the inherent noise of the thermometer bridge. It is indicated that the temperature stability is almost the same in both methods in the shorter time scale. These results mean that we can extend the period to keep constant temperature by ~30% with high temperature accuracy of ~10 μK rms. The improved PID method is supposed to be of great advantage especially in the range under 30 mA (≲150 G), which is comparable to the internal field of the FAA.

4. Discussion

By solving Eq. (12), dependence of the magnet current on time is derived as

$$i(t) = i_{\rm m}(t) + i_{\rm off} = \mathscr{A}\sqrt{t_0 - t} \tag{14}$$

in which t_0 is the integral constant, and $i_{\rm m}(t)$ is the actual current set by the current controller. We have determined the values of $\mathscr{A}$, t_0 and $i_{\rm off}$ in Table 2 by fitting the previously obtained curve of the magnet current like Fig. 3(c). The existence of $i_{\rm off}$ means that the internal magnetic field, b, should be considered in the low current situation. There also need a caution that the assumption of $x \ll 1$ for Eq. (9) is beginning to break in such situation. It is also possible to calculate the predicted value of $\mathscr{A}$ using the theoretical values for our FAA salt which is summarized in Table 3. It is derived that $\mathscr{A} = 0.234$–$0.270\,{\rm mA\,s^{-1/2}}$, which is similar to the experimental result. The difference between the predicted value and the experimental result is supposed to be within the uncertainties of the included values, approximation in the theory of magnetism,and the magnetic hysteresis of the FAA salt. Finally, we can predict the maximum control time, $t_{\rm max}$, by solving Eq. (14) as,

$$t_{\rm max} = \frac{\{i_{\rm m}(t) + i_{\rm off}\}^2 - i_{\rm off}^2}{\mathscr{A}^2} \tag{15}$$

assuming $i_{\rm m}(t + t_{\rm max}) = 0$. This technique is very useful in the actual experiments.

Acknowledgements

This research was partially supported by the Ministry of Education, Culture, Sports, Science and Technology of Japan, Grants-in-Aid for Scientific Research 16340077.

References

[1] Y. Ishisaki, et al., Proc. SPIE 5501 (2004) 123.
[2] D. McCammon, et al., Astrophys. J. 576 (2002) 188.
[3] R.L. Kelley, et al., Proc. SPIE 3765 (1999) 114.
[4] K. Shinozaki, et al., Rev. Sci. Instrum., submitted.
[5] K.D. Irwin, Ph.D. Thesis, Stanford University, 1995.
[6] C. Enss, et al., J. Low Temp. Phys. 121 (2000) 137.
[7] O.V. Lounasmaa, in: Adiabatic Demagnetization of a Paramagnetic Salt in Experimental Principles and Methods Below 1 K, Academic Press, 1974, p. 82 (Chapter 5).
[8] G. Bernstein, S. Labov, D. Landis, N. Madden, I. Millet, E. Silver, P. Richards, Cryogenics 31 (1991) 99.